Experimental study of the hydrogen complexes in indium phosphide

R. Darwich and B. Pajot
Groupe de Physique des Solides, Tour 23, Université Denis Diderot, 2 place Jussieu, 75251 Paris Cedex 05, France

B. Rose and D. Robein
France Telecom, Centre National d'Etudes des Télécommunications, 196 avenue Henri Ravera, Boîte Postale 107, 92225 Bagneux Cedex, France

B. Theys
Laboratoire de Physique des Solides, CNRS, 1 place A. Briand, 92195 Meudon Cedex, France

R. Rahbi
Groupe de Physique des Solides, Tour 23, Université Denis Diderot, 2 place Jussieu, 75251 Paris Cedex 05, France

C. Porte and F. Gendron
Laboratorie AOMC, UPMC, 4 place Jussieu, 75252 Paris Cedex 05, France
(Received 25 June 1993)

The structure of the H-related complexes in *p*-type InP and in liquid encapsulated Czochralski semi-insulating InP:Fe has been studied from the vibrational absorption of their PH stretching modes. The acceptor complexes are produced by plasma hydrogenation so that PD modes have been investigated also. The study has first been performed at 6 K on the fundamentals and on the most intense of the first overtones. The trends in the frequencies and widths of the PH modes of the H-acceptor complexes for Be, Zn, and Cd acceptors are discussed and explained qualitatively. In InP:Fe, the PH intrinsic modes are sharper than those of the acceptor complexes indicating a weaker interaction with the environment. This study has been followed by the measurement of the temperature dependence of the frequencies and of the linewidths for increasing temperatures. The frequency shifts and the broadenings of the lines are interpreted by the temperature-dependent random dephasing of the vibration of the high-frequency oscillators in the excited state. The analysis shows that the PH mode in the acceptor complexes couples to TA phonons of the InP lattice while the one in the complexes involving a vacancy couples to a two TA phonon combination. The anharmonicity of the P-H bonds is comparable to the one in phosphine. A comparison of the anharmonicity parameters derived from the overtone measurements with those derived from the hydrogen isotope effects gives evidence of the interaction between the H atom and the lattice. The amplitude of vibration of the D atom is smaller than that of the H atom and this explains why the interaction of the D atom with the lattice is smaller. This is the reason why the width of the PD modes is smaller than that of the corresponding PH modes. The splitting of some of the PH lines in samples subjected to a uniaxial stress has been studied. The splitting of the PH;Zn mode is in full agreement with a P-H bond along a ⟨111⟩ axis. The same ⟨111⟩ orientation of the P-H bond is also found from the splitting of a line attributed to an In vacancy "decorated" by a H atom (V_{In}(PH)). The splitting of the strongest line in InP:Fe leads to its attribution to a PH mode in a cubic center containing four H atoms ($V_{In}(PH)_4$). The presence of this center seems to account for most of the hydrogen present in InP:Fe. Upon annealing of the InP:Fe samples, $V_{In}(PH)_4$ is a source of atomic hydrogen that can be trapped by other defects and it can leave partially hydrogenated In vacancies.

I. INTRODUCTION

In semiconductors, H complexes can form under appropriate conditions with many shallow dopants as well as with native defects.[1] These complexes generally neutralize the electrical activity of the dopants, but the electrical properties of the H complexes with native defects depend on the electrical activity of the defect itself. These complexes are characterized by one, or less frequently, several *X*-H bonds where *X* can be an atom of the crystal or a foreign atom. Reasonable models of the structure and chemical nature of H-dopant complexes have been provided using vibrational spectroscopy at low temperature and perturbed angular correlation (PAC).[2–4] The identity of the hydrogen complexes with native defects is not so clear, even when their symmetry is known. More information is gained from a comparison of the trends in the properties of hydrogen complexes differing in the chemical nature of the dopant with those of unknown complexes. Another direction is a study of the interaction of the complex with the surrounding crystal. It manifests itself by a vibrational linewidth varying

from one center to the other and by the broadening and shift of the vibrational modes with temperature. A third way is to study the effect of an external perturbation on the samples. We present experimental results on the PH and PD stretching mode of H-acceptor and H-native defect complexes in InP and on their temperature dependences. The temperature effects are interpreted in the framework of the random vibrational dephasing model.[5,6] We have also investigated the anharmonicity of the modes from the observation of some overtones and from hydrogen isotopic substitution. We have studied the symmetry of the complexes by performing spectroscopic measurements under uniaxial stress and we have tried to correlate all the data to improve our picture of the H complexes in semiconductors.

II. EXPERIMENT

A. The materials

The InP:Zn layers investigated (~ 5 μm) were produced by metal-organic vapor-phase epitaxy (MOVPE) on thick (1.5–2.0 mm) (100)- or (110)-oriented InP:Fe substrates. The Zn doping level ($\sim 3\times 10^{18}$ at./cm^3) was measured by secondary ion mass spectroscopy (SIMS). The concentration of H-Zn complexes in the as-grown samples was about 1.5×10^{18} cm^{-3}. The 3-μm-thick InP:Be layer ($p\sim 3\times 10^{17}$ cm^{-3}) and the 5-μm-thick InP:Cd layer with $p\sim 2\times 10^{18}$ cm^{-3} were grown, respectively, by molecular beam epitaxy (MBE) and by liquid phase epitaxy (LPE) on semi-insulating (SI) InP:Fe substrates. One liquid encapsulated Czochralski (LEC) grown InP:Cd sample with $p\sim 5\times 10^{18}$ cm^{-3} was also used. All these samples were capped with a thin layer of $Ga_{0.47}In_{0.53}As$:Zn lattice-matched to InP to prevent dissociation under direct exposure to plasma.[7] Hydrogen was diffused by exposure to a H or D rf plasma (15.36 MHz). Typical conditions were a power density of 0.08 W cm^{-2} with a sample temperature of 200 °C for 6 h.

InP:Fe substrates or samples were cut in the seed end (cone) of a nominally SI LEC crystal (crystal 1) with [Fe] $\sim 2\times 10^{16}$ at./cm^3. To simulate the annealing of the substrates during the MOVPE growth, InP:Fe samples were annealed at 600 °C or 650 °C under a phosphorus pressure of one atmosphere in a quartz ampule for 3 h. SI samples cut from the cones of other crystals (2 and 3) were also measured. One InP:Fe sample (No. 4) was also studied. The samples for the uniaxial stress study were oriented by x rays to better than 1°.

B. The setup

The samples were cooled in Oxford Instruments Model Nos. CF204 or CF1204 cryostats and the spectra obtained with a Bomem Model No. DA8 Fourier-transform spectrometer at resolutions of 0.1 or 0.013 cm^{-1} near liquid helium temperature (LHeT). The CF1204 cryostat, equipped with one Rh/Fe temperature sensor in the cryostat and one Rh/Fe sensor in the sample holder, was used for the measurements as a function of temperature. In the CF204 cryostat, the temperature of the sample was deduced from the temperature of the manganin temperature sensor in the heat exchanger. The CF204 could be fitted with a spring-loaded stress system built at the Laboratoire AOMC. In this stress system, the force applied to the piston is read from a transducer at room temperature. The base temperature of the sample in the stress system is 8 K. Radiation was polarized by a Cambridge Instruments grid polarizer on a calcium fluoride substrate.

III. EXPERIMENTAL RESULTS

A. The LHeT results

1. The H- and D-acceptor complexes

The IR absorption of the p-type samples neutralized by hydrogen shows only one H- or D-related mode for each acceptor. The frequency and full width at half-peak (FWHP) of this mode at 6 K for different acceptors are given in Table I. The frequencies show an acceptor dependence, but the average is comparable to the frequencies of the PH stretching mode in phosphine.[8] On the other hand, they are rather different from Be-H, Zn-H, or Cd-H stretching frequencies in diatomic molecules.[9] From these two facts we were first led to attribute the modes observed to PH bonds perturbed by the acceptor atom with only one such bond per acceptor complex.[10] We denote these modes as follows: PH; Be, PH;Zn, PH;Cd, etc.

The FWHP's depend on the nature of the acceptor. The same trend is also observed for the H complexes with group-II acceptors in GaAs.[11] The FWHP's for the D

TABLE I. Measured position and FWHP (cm^{-1}) at 6 K of the fundamentals (ω_1) and overtones (ω_2) of some hydrogen-acceptor complexes in InP and GaAs. I_2/I_1 is the experimental overtone-fundamental intensity ratio.

Mode	ω_1	FWHP	ω_2	FWHP	I_2/I_1
PH;Be	2236.49	0.43			
PD;Be	1630.85	0.2			
PH;Zn	2287.71	0.23	4487.80	0.56	0.009
PD;Zn	1664.52	0.08	3283.34	0.14	0.007
PH;Cd	2332.42	0.12	4580.20	1.0	0.006
PD;Cd	1695.40	0.10			
AsH;Zn	2146.94	1.8	4216.7	3.7	0.005
AsD;Zn	1549.05	0.9			

complexes are smaller than those of the corresponding H complexes and this difference is related to the mass dependence of the amplitude of vibration of the hydrogen atom. For this reason, the intensities of the PD modes are weaker than those of the corresponding PH modes for the same concentrations.

The first overtones of the PH;Zn, PD;Zn, and AsH;Zn modes have already been reported[12] and those of the PH;Cd modes have also been observed. The ratio of the intensity of the first overtone to the fundamental is ~ 0.01 or less. The positions and FWHP's of the overtones are given in Table I with the ratio I_2/I_1 of the intensities of the overtone to the fundamental. The integrated intensity of the PH mode is proportional to the Zn concentration. The optical calibration coefficient between the concentration of H-Zn complexes and the integrated intensity I of the mode is given by

$$[\text{H-Zn}](\text{cm}^{-3}) = (2.0 \pm 0.2) \times 10^{16} I_{[\text{H-Zn}]}(\text{cm}^{-2}) \ .$$

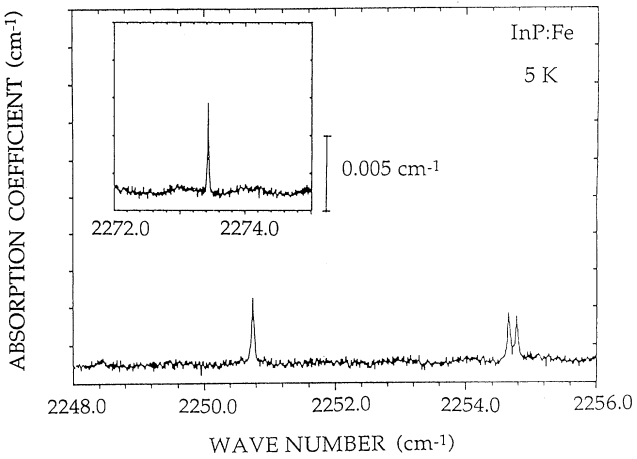

FIG. 1. Absorption of PH modes produced in a sample from crystal 1 by annealing at 600 °C. The resolution is 0.013 cm^{-1}.

2. *The H modes in InP:Fe*

Many lines in the 2200–2300-cm^{-1} spectral region are observed in InP:Fe. They are globally attributed to PH stretching modes in different complexes.[2] In the samples studied, some lines were observed only after annealing at 600 °C or 650 °C and they are noted with an asterisk in Table II. All the H-related lines in InP:Fe are weak except that at 2316 cm^{-1}. Some of the lines of Table II were observed only in one sample. They reflect the occurrence of intrinsic H-related complexes and of residual H-impurity complexes that can differ from one sample to the other. The line at 2250 cm^{-1} and the 2254-cm^{-1} doublet are observed with the same intensity ratio in the samples investigated (Fig. 1). They are observed in all the InP:Fe samples under appropriate conditions and should be related to intrinsic centers. The lines at 2306, 2307, and 2311 cm^{-1} shown in Fig. 2 have been observed for the first time in samples 1, 2, and 3 and they could be related to one or more extrinsic centers. The line at 2288 cm^{-1} is due to a PH;Zn mode.[10] The presence of Zn as a residual impurity in InP:Fe has been noted previously[2] and from the above calibration coefficient, the concentration of residual Zn complexes in sample 1 is $\sim 3 \times 10^{14}$ cm^{-3}. In LEC SI InP:Fe samples, the existence of (H,Fe) complexes has not yet been established. The line at 2285.7 cm^{-1} could be related to such complexes,[13] but its occurrence would be Fermi-level dependent.

The presence of complexes with the heavy Hg acceptor is not excluded and they could be related to the weak lines at 2322 or 2333 cm^{-1}. The line at 2316 cm^{-1} is especially intense and it was possible to observe its first overtone with an intensity ratio of 0.004 (Fig. 3). In the as-grown samples, the 2203-cm^{-1} line and other weak H-related lines were not observed. They appeared only after annealing at 600 °C or above or in the substrates of the InP:Zn layers. This could be due to the growth conditions or to the location of the samples in the crystal as the 2202-cm^{-1} line has been seemingly observed in other as-grown samples. This line has been previously as-

TABLE II. Position and FWHP (cm^{-1}) at 6 K of lines in the spectral domain of the PH modes in the SI InP:Fe samples investigated (Nos. 1, 2, 3, and 4). Some of these lines have been previously reported in Ref. 2. The asterisks denote lines observed after annealing. Attributions are given in parentheses. The overtone of the line at 2316 cm^{-1} is observed at 4547.49 cm^{-1}. Its FWH is 0.04 cm^{-1} and its intensity with respect to the fundamental is 0.004.

Position	FWHP	Remarks	Position	FWHP	Remarks
2332.90	~ 0.3	Weak, No. 1	2287.71	0.23	Ref. 2, Nos. 1 and 4 (PH;Zn)
2322.12	~ 0.3	Weak, No. 2	2285.69	0.12	Ref. 2, Nos. 2 and 3
2315.62	0.03	Ref. 2	2282.8*	~ 1	Ref. 2
2311.27	0.09	Medium	2273.43*	0.07	Ref. 2
2307.27	0.05	Medium	2254.78*	0.05	Ref. 2
2306.83	0.04	Medium	2254.65*	0.05	Ref. 2
2304.15	~ 0.1	Weak, No. 2	2250.76*	0.05	Ref. 2
2303.18	~ 0.1	Weak, No. 2	2236.19*	~ 0.1	Weak, No. 1
2302.54		Weak, No. 2	2202.39*	0.015	Ref. 2 (V_{In}(PH))

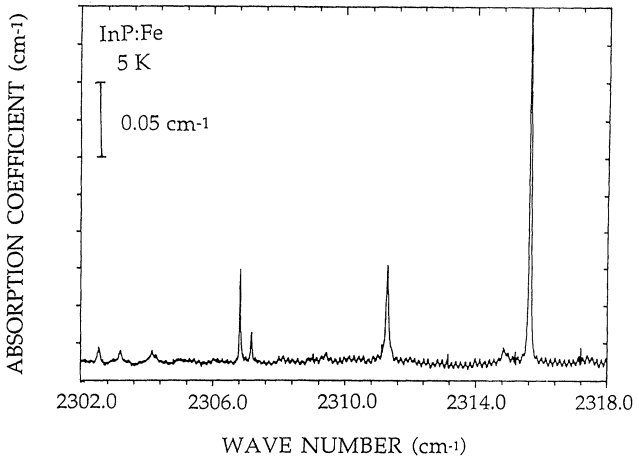

FIG. 2. Absorption of PH modes related to native complexes in a sample from as-grown crystal No. 2. The lines near 2307 and 2311 cm^{-1} are also observed in samples from crystals 1 and 3. The peak intensity of the line at 2316 cm^{-1} (truncated) is 12.4 times that of the line near 2311 cm^{-1}. The resolution is 0.013 cm^{-1}.

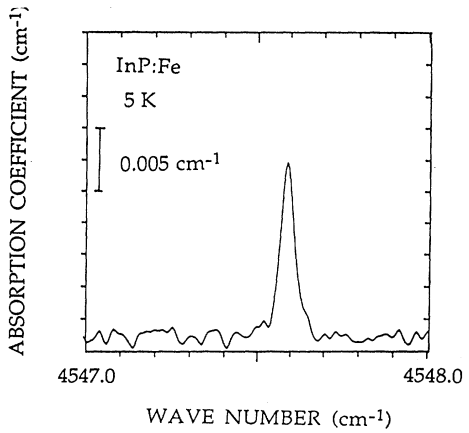

FIG. 3. Overtone of the PH mode at 2316 cm^{-1}. The resolution is 0.02 cm^{-1}.

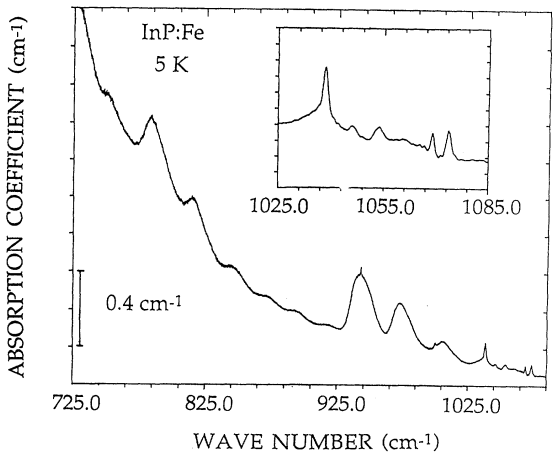

FIG. 4. Absorption at 6 K (resolution 0.1 cm^{-1}) in a sample from crystal 2 in the three-phonon region of InP. Note the lines at 942.6 and 999.9 cm^{-1}. The inset (resolution 0.4 cm^{-1}) shows the 1050-cm^{-1} region. The most intense lines are at 1038.5, 1068.9, and 1073.6 cm^{-1}.

cribed[14] to an In vacancy (V_{In}) "decorated" by a single H atom. It is labeled here V_{In}(PH). Weak lines were also observed in the PH bending frequencies region[8] (Fig. 4). Those near 1050 cm^{-1} are related to at least two different centers. One set is observed in all the InP:Fe samples. They seem to have a vibrational origin. The lines at 942.7 and 999.9 cm^{-1} were observed in sample 2. There seems to be no relationship between these lines and those in the 2200–2340-cm^{-1} region so that they cannot be attributed to PH bending modes.

B. Temperature dependence of the H-related modes

1. The H- and D acceptor complexes

When temperature is raised from LHeT, the PH; acceptor modes shift to lower frequencies and broaden as shown in Fig. 5(a) for the PH;Cd mode. The modes are barely discernible above 150 K; however, no satellite line like the one for SiH;Al and SiH;Ga in silicon[15] is observed when temperature is increased. Figure 6 shows the temperature dependence of the FWHP's and of the position of the PH;Zn, PD;Zn, and PH;Cd modes. The solid lines correspond to fits that will be discussed later.

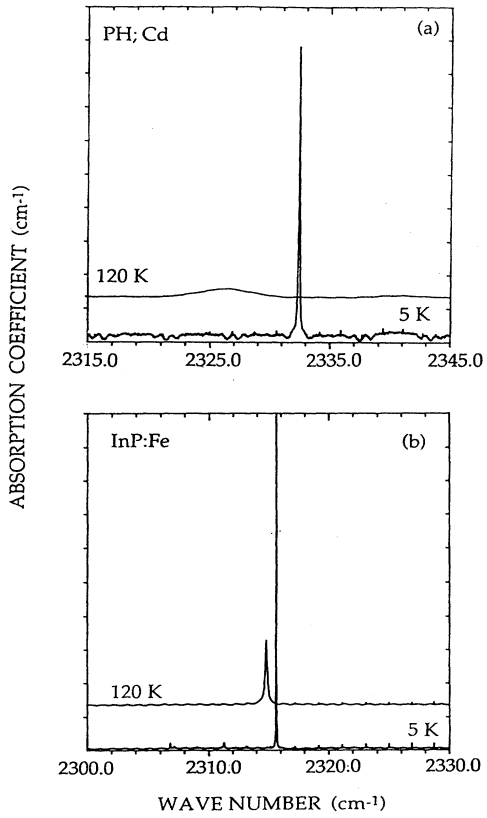

FIG. 5. Difference between the temperature dependences of two PH modes: (a) the PH;Cd mode in InP:Cd and (b) the PH mode of the 2316-cm^{-1} line in InP:Fe.

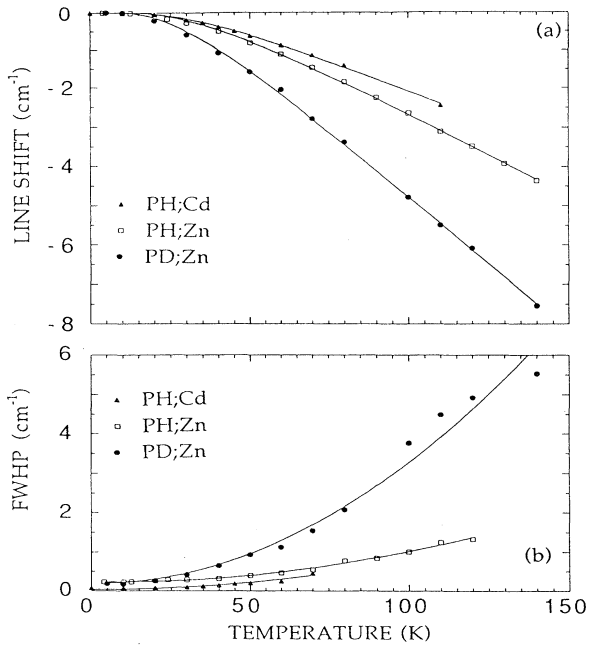

FIG. 6. (a) Acceptor and hydrogen isotope dependence of the temperature shift of the P-hydrogen modes of (acceptor-hydrogen) complexes in InP. (b) The same for the FWHP (cm^{-1}). The solid lines are three-parameter fits using the random vibrational dephasing model.

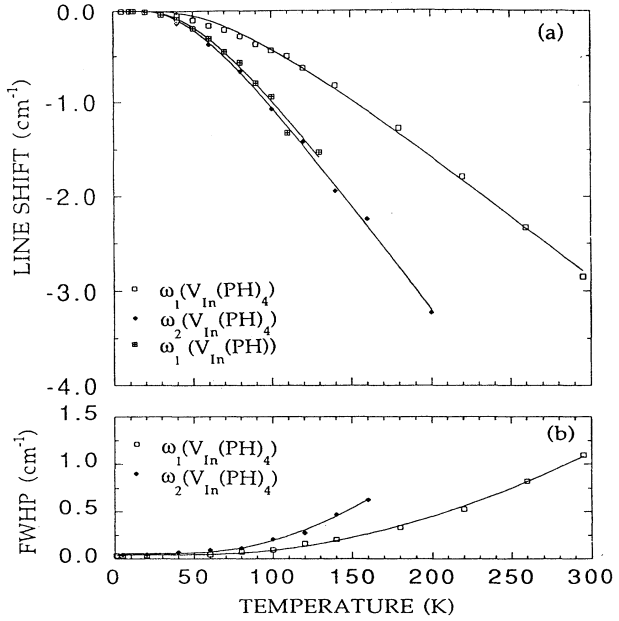

FIG. 7. (a) Shift with temperature of the V_{In}(PH) mode and of the fundamental (ω_1) and overtone (ω_2) frequency of the PH mode in $V_{In}(PH)_4$ (the 2316-cm^{-1} line). (b) The same for the FWHP's. The solid lines are three-parameter fits using the random vibrational dephasing model.

The broadening (like the FWHP at LHeT) is acceptor dependent and reflects the interaction of the H atom with the lattice. For instance, the FWHP of the PH;Cd mode at 6 K is smaller than that of the PH;Zn mode (0.17 and 0.23 cm^{-1}, respectively) but at 120 K, the order is inverted (4.9 and 2.2 cm^{-1}, respectively). The shifts are small up to ~20 K and at high temperature they are practically linear with temperature. There is a correlation between the shift and the broadening of the modes and the amplitude of vibration as evidenced by the smaller values measured by PD;Zn compared to PH;Zn.

2. *The H modes in InP:Fe*

The shift and broadening of these modes with temperature are smaller than those for the PH; acceptor modes [Fig. 5(b)]. The shift of the line at 2316 cm^{-1} is shown in Fig. 7(a). The shift of the overtone at 4548 cm^{-1}, also shown in this figure, is about twice as large as that of the fundamental. This is related to the amplitude of vibration of the H atom. The temperature dependences of the FWHP's of the fundamental and of the overtone [Fig. 7(b)] show the same trend. The shift with temperature of the V_{In}(PH) mode is comparable to that of the line at 2306.8 cm^{-1}. Exceptions are the lines at 2251 and 2306.9 cm^{-1} that broaden rapidly and cannot be observed in our samples above 40 K. The lines near 2250 cm^{-1} shown in Fig. 1 have a *positive* temperature shift. A similar observation has been made for some OH and NH modes in GaAs.[16]

C. Piezospectroscopic results

1. *The PH;Zn mode*

a. Stress along [100]. The frequency of the mode shifts with stress and no polarization effect is observed, as seen in Fig. 8.

b. Stress along [110]. When the propagation vector **k**

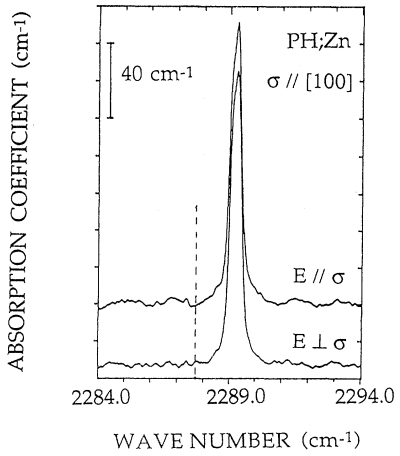

FIG. 8. Shift of the PH;Zn mode at 8 K for a stress of 400 MPa applied along a ⟨100⟩ direction. The line for $\mathbf{E}\|\sigma$ has been displaced for clarity. The FWHP's are 0.5 cm^{-1}. No significant difference is observed between the two polarizations. The dotted line is at the zero-stress frequency of the mode.

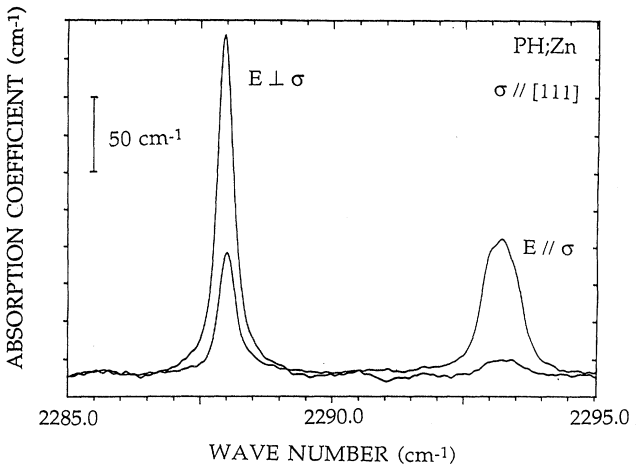

FIG. 9. Splitting of the PH;Zn mode at 8 K for a stress of 273 MPa applied along a ⟨111⟩ direction. The resolution is 0.1 cm^{-1}. A small misorientation of the polarizer is responsible for the observation of the weak high-energy component for $\mathbf{E}\perp\sigma$.

of the radiation is along [001], the mode splits with stress into two fully polarized components (the high- and low-energy components, respectively, are $\mathbf{E}\|\sigma$ and $\mathbf{E}\perp\sigma$).[17] Their splitting is (10.4 ± 0.9) cm^{-1}/GPa. The ratio of the intensities of the two components is near unity. For a stress of ~0.3 GPa, the FWHP of the $\mathbf{E}\perp\sigma$ component is the same as that at zero stress, but the FWHP of the $\mathbf{E}\|\sigma$ component is about two times larger. For the D isotope, the qualitative features are the same as those for H, but the splitting reduces to (7.5 ± 0.7) cm^{-1}/GPa. The ratio of the splittings of the PH and PD modes (1.39) is comparable to the ratio of the corresponding frequencies as expected for a mode involving primarily the motion of a hydrogen atom. For $\mathbf{k}\|[1\bar{1}0]$, two components of comparable intensity are observed for $\mathbf{E}\perp\sigma$.

c. Stress along [111]. The mode splits into two components (Fig. 9). For $\mathbf{E}\|\sigma$, the measured ratio of the intensities of the high- to low-energy component is ~3.0. Their splitting is (15.0 ± 1.3) cm^{-1}/GPa.

These results were obtained at 8 K and they are summarized in Fig. 10. A measurement performed at 75 K for $\sigma\|[110]$ produced comparable splitting coefficients. The reorientation energy of the P-H bond of the PH;Zn center among the four equivalent orientations has been measured from the temperature-dependent annealing of the stress-induced dichroism. This energy is 0.8 eV, assuming that the recovery is a first-order process.[17]

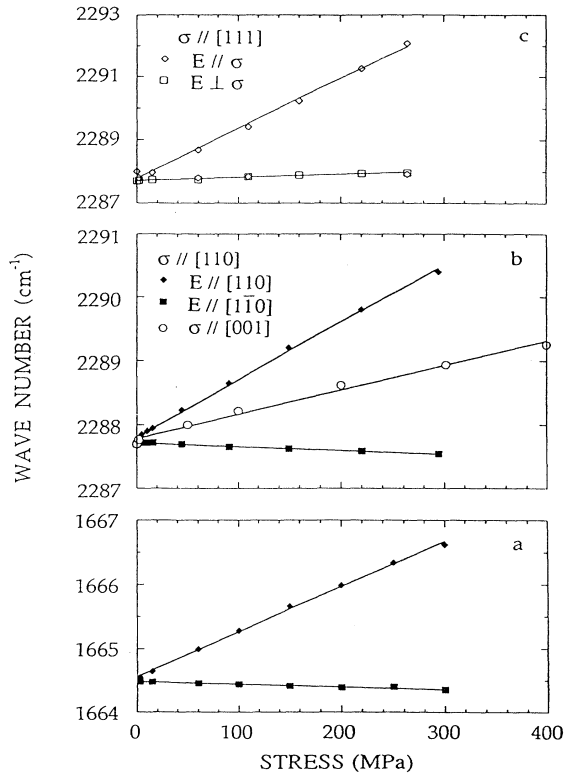

FIG. 10. Shift with stress at 8 K of (a) the components of the PD;Zn mode for $\sigma\|[110]$, and $\mathbf{k}\|[001]$, (b) the components of the PH;Zn mode for $\sigma\|[110]$ ($\mathbf{k}\|[001]$) and $\sigma\|[100]$, and (c) the components of the PH;Zn mode for $\sigma\|[111]$ (ordinate scale divided by 2).

2. *The PH-related lines in SI InP:Fe*

The effect of uniaxial stress has been studied in detail for the V_{In}(PH) mode and for the 2316-cm^{-1} lines. The effect of a stress splitting on the V_{In}(PH) mode has been previously mentioned.[2]

a. Stress along [100]. As shown in Fig. 11(a), the V_{In}(PH) mode shifts with a negative slope and no polarization effect is observed. For the 2316-cm^{-1} line, a small splitting is observed that is beyond experimental

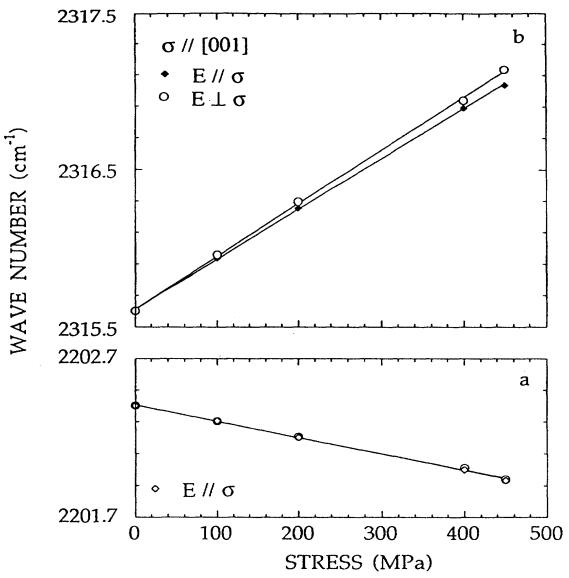

FIG. 11. Shift with stress at 8 K of PH modes in InP:Fe for $\sigma\|[001]$: (a) The V_{In}(PH) mode. No detectable splitting is observed between the two polarizations within experimental accuracy. (b) For the 2316-cm^{-1} line, two components are observed under the same conditions. The resolution is 0.1 cm^{-1} for (a) and (b).

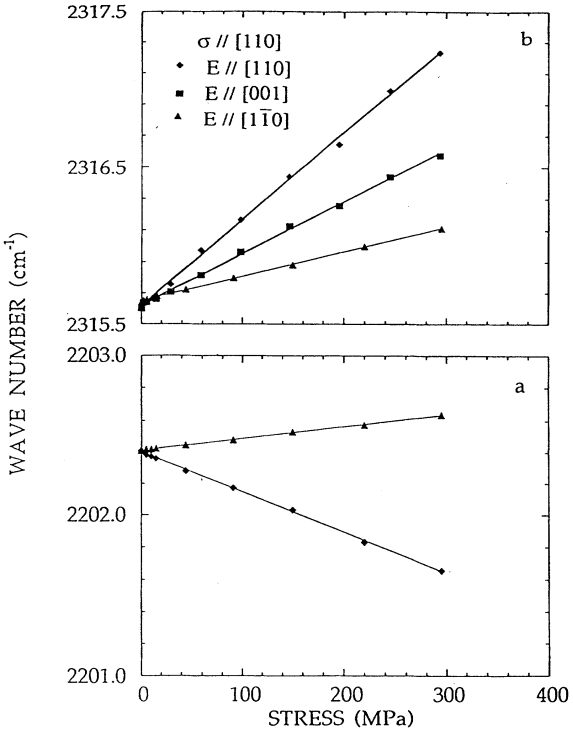

FIG. 12. Shift with stress at 8 K of PH modes in InP:Fe for $\sigma \| [110]$: (a) The V_{In}(PH) mode for $\mathbf{k} \| [001]$. (b) The 2316-cm^{-1} line for $\mathbf{k} \| [001]$ and $\mathbf{k} \| [1\bar{1}0]$.

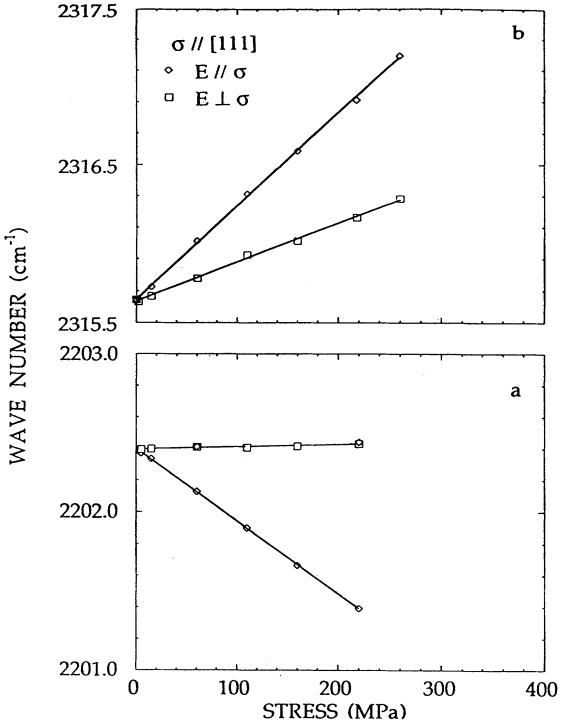

FIG. 14. Shift with stress at 8 K of PH modes in InP:Fe for $\sigma \| [111]$: (a) The V_{In}(PH) mode and (b) the 2316-cm^{-1} line.

uncertainty and the slope of the $\mathbf{E} \perp \sigma$ component is larger than that of the $\mathbf{E} \| \sigma$ component [Fig. 11(b)].

b. Stress along [110]. The V_{In}(PH) mode splits into two components and their polarizations are the same as those for the PH;Zn mode, but the high-energy component is observed for $\mathbf{E} \perp \sigma$ (Fig. 12). For $\mathbf{k} \| [001]$, the 2316 cm^{-1} line also splits into two fully polarized components. For $\mathbf{k} \| [1\bar{1}0]$, this line splits *again* into two fully polarized components but the one for $\mathbf{E} \perp \sigma$ is a new component with a stress dependence that is intermediate between those of the components for $\mathbf{k} \| [001]$ (Fig. 11). The polarization-dependent splitting of the 2316-cm^{-1} line is shown in Fig. 13.

c. Stress along [111]. The two lines split into two components (Fig. 14). There, again, a difference is found between the V_{In}(PH) mode and the 2316-cm^{-1} line, as for the latter, the two components are fully polarized. No dichroism is observed for the 2316-cm^{-1} line and for the V_{In}(PH) mode when the stress is applied at room temperature and the sample cooled under stress.[18]

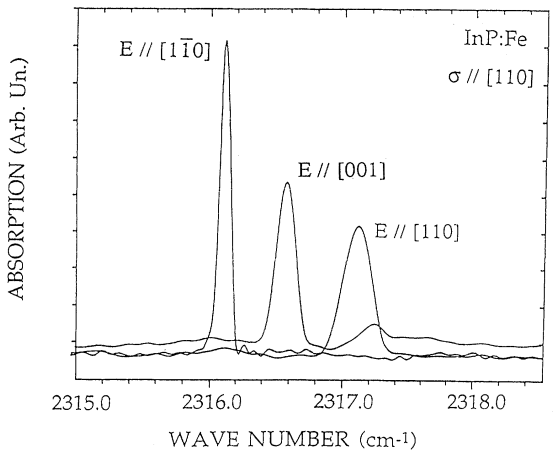

FIG. 13. Splitting of the 2316-cm^{-1} line at 8 K for $\sigma \| [110]$. For $\mathbf{E} \| [110]$ and $\mathbf{E} \| [1\bar{1}0]$, the stress is 293 MPa. For $\mathbf{E} \| [001]$, the stress is 295 MPa.

IV. DISCUSSION

A. The frequencies and the linewidths at 6 K

1. The H-acceptor complexes in GaAs and InP

The frequencies of the H modes indicate that the H atom of the acceptor complex is mainly bonded to a group-V atom. The most probable location of the H atom is then between the group-V atom and the acceptor. This location is called bond centered (BC) and it explains the neutralization of the acceptors.[19,20] With this location, the observed increase of the frequency of the H mode with the size of the acceptor atom is explained by some kind of confinement of the H bond by the acceptor.

The FWHP of the PH; acceptor modes decrease from PH;Be to PH;Cd. The width of the PH mode must depend on the interaction between the H atom and the acceptor. This interaction can be translated into a weak

force constant between the two atoms. It can depend on (i) the distance between the H atom and the acceptor, (ii) the amplitude of vibration of the H atom, and (iii) the electronic interaction between the acceptor and the H atom. It seems that the H-acceptor distance alone does not play an important role in the broadening of the mode. If this were the case, we would expect the PH;Cd mode to be the broadest because the confinement is the strongest for this pair. Now this mode is the sharpest (Table I). The interaction between H and the acceptor would certainly be reduced if the P-H bond was pushed out from the ⟨111⟩ direction to reduce the interaction between the H atom and the acceptor. This displacement, however, would reduce the frequency of the mode by reducing the confinement of the H atom; it is also possible that hindered rotation of the P-H bond about the ⟨111⟩ axis would produce temperature-dependent satellites. These two consequences are against the experimental evidence and we conclude that the P-H bond remains along the ⟨111⟩ axis. The last cause lies in the electronic properties of the acceptor or in its difference of electronegativity with H. A correlation can be made between the FWHP of the PH; acceptor mode and the binding energy of the H-acceptor molecule. For these diatomic molecules it is found[9] that the binding energy decreases from H-Be to H-Cd. This interaction decreases in the same direction as the FWHP of the PH modes. From this, we are led to assume that the low-temperature FWHP of the PH; acceptor modes is mainly related to the electronic affinity between the H and acceptor atoms and not to a steric effect due to the size of the acceptor.

To summarize, from the above results it seems that the frequency of the modes is related to the size of the acceptor atoms through a small change of the P-H bond length. The larger the size of the acceptor, the smaller the bond length and the higher the frequency. The FWHP of the modes seems to be controlled by the electronegativity difference (or by the screening) between the H and the acceptor atoms. The increase of the screening from Be to Cd can thus explain why the PH;Cd lines are sharper than the PH;Be lines.

B. Discussion of the uniaxial stress results

1. The [H,Zn] complex

When compared to the splitting expected for different defect orientations in cubic crystals,[21] it is found that the patterns observed for the PH;Zn mode match quantitatively an orientation of the P-H bond along a ⟨111⟩ trigonal axis. This result provides another physical basis to the initial H complex model. For this symmetry, the four equivalent orientations of the P-H dipoles are labelled I, II, III, and IV for [111], $[\bar{1}\,\bar{1}\,1]$, $[\bar{1}1\bar{1}]$, and $[1\,\bar{1}\,\bar{1}]$, respectively. For a stress in a (110) plane making an angle θ with the [001] axis, the splitting δ per unit stress of the modes with different orientations can be expressed by two piezospectroscopic parameters A_1 and A_2:

$$\begin{aligned}\delta_{\mathrm{I}}(\theta)&=A_1+A_2\sin\theta(\sin\theta+2\sqrt{2}\cos\theta)\ ,\\ \delta_{\mathrm{II}}(\theta)&=A_1+A_2\sin\theta(\sin\theta+2\sqrt{2}\cos\theta)\ ,\\ \delta_{\mathrm{III}}(\theta)&=\delta_{\mathrm{IV}}(\theta)=A_1-A_2\sin^2\theta\ .\end{aligned}\tag{1}$$

The average values of the parameters A_1 and A_2 for the PH;Zn mode are close to the ones reported before.[17] For the AsH;Be mode in GaAs, values of 5.0 and 6.5 cm^{-1}/GPa for A_1 and A_2 were reported[22] and for Si-H; B, larger coefficients were found ($A_1=12.7$ cm^{-1}/GPa and $A_2=13.5$ cm^{-1}/GPa).[23] It is found that the frequency of the PH bond parallel to the stress increases. This is consistent with a small reduction in the P-H bond length when the H and Zn atoms are pushed against each other. This produces an increase of the interaction between these two atoms which must also be one cause of the broadening of the components for $\mathbf{E}\|\sigma$. The reorientation energy of the P-H bond of the PH;Zn center (0.8 eV) is notably higher than the one for AsH;Be in GaAs (0.4 eV) or for SiH;B in silicon (0.2 eV). A crude correlation can be made with the H-acceptor distance and the H-acceptor electronegativity difference in these three semiconductors. It seems to show that the higher the H-acceptor interaction, the lower the reorientation energy.

2. The 2316-cm^{-1} line and the V_{In}(PH) mode

The stress behavior of the 2316-cm^{-1} line is different from that for a singly degenerate stretching mode with trigonal symmetry. Its splitting and polarization characteristics are similar to the ones for a SiH mode at 2223 cm^{-1} in proton-implanted silicon.[24] For this SiH mode, no splitting is observed for $\sigma\|[100]$. For $\sigma\|[110]$ and $\mathbf{k}\|[1\bar{1}0]$, the line splits into two fully polarized components and a third component for $\mathbf{k}\|[001]$ has also been observed.[25] For $\sigma\|[111]$, two fully polarized components are observed. The 2223-cm^{-1} line is also observed in silicon growth in a H_2 atmosphere. In silicon growth in a H_2+D_2 atmosphere, four new lines are observed in the same spectral region.[26] They are ascribed to Si-H bonds whose frequencies are perturbed by Si-D bonds in a center with several equivalent Si-H bonds: when the H atom of one of these bonds is replaced by a D atom, the symmetry and the environment are changed and the frequencies are altered. The coimplantation of silicon with protons and deuterons reveals the presence of another new line near 2223 cm^{-1} not seen in silicon implanted only with protons.[24] The existence of six different SiH stretching frequencies associated with this center in samples containing H+D suggests a combination of Si-H and Si-D bonds corresponding to a center with tetrahedral symmetry containing four Si-H bonds. It could be an interstitial SiH_4 (silane) molecule or a vacancy "decorated" by four H atoms ($V(SiH)_4$). It must be pointed out that no bending mode of the Si-H bond related to this center has been reported.

Centers with cubic symmetry containing four equivalent X-H bonds are analogous to spherical tops XH_4 molecules.[27] Two different XH stretching modes are expected: a symmetric Raman active "breathing" mode and a triply degenerate mode that is infrared and Raman

active. The stress-induced shifts and splittings of a triply degenerate mode for a cubic center in a semiconductor with diamond or zinc-blende structures are given in Table III for simple stress directions. They are expressed as functions of A, B, and C that are piezospectroscopic parameters similar to A_1 and A_2 for the trigonal defects. In the present case, however, the stress splitting is related to vibrational degeneracy and there is no orientational degeneracy. A treatment of the effect of a uniaxial stress on the XH stretching force constants for a center with tetrahedral symmetry is made in Ref. 24. It is based on the harmonic approximation but it is valuable as it provides a more direct insight than the phenomenological model using the piezospectroscopic parameters. The change of the effective force constant of one of the four XH bonds of the center (i, for definiteness) for a stress along a $[hkl]$ direction is

$$f_i^{[hkl]}=f_{\parallel}\cos^2\theta+f_{\perp}\sin^2\theta\ , \tag{2}$$

where $f_{\parallel}$ and $f_{\perp}$ are the changes in the effective force constant for a stress parallel or perpendicular, respectively, to the direction of the bond and θ is the angle between bond i and the direction $[hkl]$. By comparing the perturbation induced by the uniaxial stress through the change of the force constants and the piezospectroscopic parameters, it is found that A and C are proportional to $(f_{\parallel}+2f_{\perp})/6$ and $(f_{\parallel}-f_{\perp})/3$, respectively, and that $B=0$. In Table III, the splitting between the two components for $\sigma\|[001]$ is $3B\sigma$ and this correlates with the absence of splitting of the 2223-cm^{-1} line in silicon for that orientation of the stress.

If it is assumed that the 2316-cm^{-1} line in InP:Fe is due to the triply degenerate PH mode of a $V_{\rm In}(PH)_4$ center, the consequences are (i) no splitting for $\sigma\|[001]$, (ii) the same value of the splitting ($C\sigma$) for $\sigma\|[111]$ and between the $\mathbf{E}\|[110]$ and $\mathbf{E}\|[1\bar{1}0]$ components for $\sigma\|[110]$, (iii) three fully polarized components for $\sigma\|[110]$, and (iv) full polarization of the components for $\sigma\|[111]$. Experimentally, a very small splitting is observed for $\sigma\|[001]$ (Fig. 11) from which $B=-0.06$ cm^{-1}/GPa is obtained. This splitting can be due to the small anharmonicity measured for the PH bond. The splittings measured for $\sigma\|[111]$ and between the $\mathbf{E}\|[110]$ and $\mathbf{E}\|[1\bar{1}0]$ components for $\sigma\|[110]$ are 3.4 and 3.3 cm^{-1}/GPa, respectively. The experimental data show that, for $\sigma\|[110]$, three components are indeed observed with the expected polarizations (Fig. 12) and that, for $\sigma\|[111]$, the two components are fully polarized (Fig. 14). These observations seem to show that the 2316-cm^{-1} line is due to the triply degenerate PH stretching mode of a $V_{\rm In}(PH)_4$ center ($V_{\rm In}(PH)_4$ mode). For a cubic center, no stress-induced dichroism is expected as no change of population is possible and no dichroism is found experimentally either for the 2316-cm^{-1} line. The similitude between the stress behaviors of the $V_{\rm In}(PH)_4$ mode in InP and the 2223-cm^{-1} line in silicon favors for the latter an attribution to a $V(SiH)_4$ center rather than to an interstitial silane molecule. The $V_{\rm In}(PH)_4$ centers are also produced by proton implantation in InP.[28,29] Coimplantation of protons and deuterons have been made in InP:Fe to try to detect PH modes in centers containing one or more P-D bonds. With the previous attribution, up to six such PH modes should be observed near 2316 cm^{-1}. The spectra of the coimplanted samples show a decrease of the intensity of the $V_{\rm In}(PH)_4$ mode, but the broadening of the vibrational lines in the implanted samples and the interference fringes due to the implanted layer prevent definitive conclusions.[29]

It has been suggested recently[30] that the 2316-cm^{-1} line was due to a normal P atom bonded to two H atoms each in a BC site with a nearest-neighbor In vacancy ($V_{\rm In2}(PH_2)$). This complex which involves some kind of split divacancy should display a C_{2v} symmetry and would produce two distinct PH stretching modes. This point and the stress splitting expected contradict experimental evidence and we discard this attribution.

The splitting of the $V_{\rm In}(PH)$ mode under a uniaxial stress indicates a P-H bond oriented along a $\langle 111\rangle$ axis with

$$A_1=(-0.9\pm0.3)\ \text{cm}^{-1}/\text{GPa}$$

and

$$A_2=(-1.8\pm0.6)\ \text{cm}^{-1}/\text{GPa}\ .$$

When the stress is applied parallel to the bond, the frequency of the corresponding mode decreases. This behavior has been observed[31] for the Si_{Ga}-H bond in hydrogenated n-type GaAs:Si. There, the H atom is in an interstitial site symmetrical from the BC site along a

TABLE III. Lifting of the vibrational degeneracy of the singlet→ triplet mode of a cubic center in a cubic crystal. The shift Δ per unit stress is expressed as a function of the piezospectroscopic parameters A, B, and C. The polarization ratios of the components for $\mathbf{E}_{\parallel}$ ($I_{\parallel}$) or $\mathbf{E}_{\perp}$ ($I_{\perp}$) to the stress is indicated.

Stress parallel to	Δ	$I_{\parallel}$:$I_{\perp}$	
[100]	$A-B$	0:1	
	$A+2B$	1:0	
[111]	$A-C/3$	0:1	
	$A+2C/3$	1:0	
Stress parallel to	Δ	$\mathbf{k}\|[1\bar{1}0]$	$\mathbf{k}\|[001]$
[110]	$A+B/2+C/2$	1:0	1:0
	$A+B/2-C/2$	0:0	0:1
	$A-B$	0:1	0:0

TABLE IV. Piezospectroscopic coefficients (cm^{-1}/GPa) at 8 K of PH modes in InP. The values in parentheses are for weak lines that seem to correspond to trigonal centers.

	Trigonal symmetry	
Mode or line	A_1	A_2
PH;Zn	4.1	5.1
PD;Zn	3.1	3.7
V_{In}(PH)	−0.9	−1.8
2306.9 cm^{-1}	(2.6)	(0.9)
2307.2 cm^{-1}	(2.7)	(1.1)
2311 cm^{-1}	(2.1)	(−0.3)

	Tetrahedral symmetry		
Mode or line	A	B	C
2316 cm^{-1}	3.5	−0.06	3.3

⟨111⟩ direction. This location is termed antibonding (AB). The stretching frequency of AB hydrogen is lower than the corresponding *BC* frequency. For a stress along ⟨111⟩, the antibonded H atom is pushed toward a tetrahedral interstitial position and the frequency is found to decrease. One of the consequences of this AB location is that the bond is free to wag at a lower frequency, giving a doubly degenerate mode. No wag mode can be related to the 2203-cm^{-1} line and this implies that the H atom of the mode is not in an AB location. This is the situation of a H atom "decorating" an In vacancy (V_{In}(PH)). This complex displays a trigonal symmetry, but the stress along the bond pushes the H atom toward the tetrahedral vacancy site so that the frequency is also expected to decrease. This structure has been proposed previously for this defect.[2]

The P-H bond of the V_{In}(PH) center can reorient since there are four equivalent orientations of the P-H bond. The absence of dichroism in this mode for stresses applied at room temperature implies a reorientation energy larger than 1 eV. The piezospectroscopic coefficients of the different centers or lines investigated are given in Table IV.

C. The anharmonicity

1. The anharmonic potential

The anharmonicity of the vibration of a chemical bond is an intrinsic property of the bond. It means that for some excitation level, the bond dissociates. For isolated diatomic molecules, the determination of the anharmonicity parameters allows an estimation of the dissociation energy. For the *X*-H bonds considered here, the situation is different because one of the atoms is bonded to atoms of the crystal and because it can be difficult for a *BC* H atom to escape along the *X*-H bond. For this reason, it seems unreasonable to derive a dissociation energy from an analysis of the low-temperature anharmonic effects observed, but we can try to obtain information on the interaction between the H bond and the lattice. We first discuss briefly the anharmonic Morse potential.[32]

For a one-dimensional oscillator with reduced mass μ vibrating at frequency ν (Hz) with amplitude x, the harmonic potential is $2\pi^2\nu^2\mu x^2$. By introducing the dimensionless variable $\xi=x/\ell$, where $\ell=\sqrt{(h/4\pi^2\mu\nu)}$, and expressing the frequency $\omega=\nu/c$ in wave-number units (cm^{-1}), the harmonic potential in cm^{-1} is $V_h(\xi)=\omega\xi^2/2$. With the preceding notation, the Morse potential is

$$V_M(\xi)=V_{eq}[1-\exp(-\alpha_M\xi)]^2-V_{eq}\ , \tag{3}$$

where the dimensionless parameter α_M is $\sqrt{(\omega_e/2V_{eq})}$. The quasiexact eigenvalues of the vibrational Hamiltonian with the potential (3) are

$$\omega_M(v)=\omega_e(v+\tfrac{1}{2})-\omega_e x_e(v+\tfrac{1}{2})^2\ , \tag{4}$$

where $x_e=\omega_e/4V_{eq}$ is an anharmonicity parameter, like ω_e and V_{eq}. The fundamental and first overtone are $\omega_1=\omega_M(1)-\omega_M(0)$ and $\omega_2=\omega_M(2)-\omega_M(0)$; hence, $\omega_e=3\omega_1-\omega_2$ and

$$x_e=(2\omega_1-\omega_2)/2(3\omega_1-\omega_2)\ .$$

The overtone-fundamental intensity ratio calculated for a Morse potential is[33]

$$(I_2/I_1)_M=x_e(1-5x_e)/(1-3x_e)^2\sim x_e \tag{5}$$

if the dipole moment is taken to be linear in ξ (no electrical anharmonicity).

2. The anharmonicity parameters deduced from the overtone data

The values of the anharmonicity parameters are given in Table V. Parameter x_e has been measured for As-H and P-H bonds in the gas phase (0.0182 and 0.0184 for dimethylarsine and dimethylphosphine, respectively[34]). The comparison with Table V seems to indicate that the bonds we are considering in the solid phase are indeed As-H and P-H bonds. An origin of the small difference between the anharmonicity of the As-H;Zn and P-H;Zn bonds in GaAs and InP can lie in the relative values of

TABLE V. Anharmonicity parameters at 6 K of some hydrogen bonds in InP and GaAs calculated from the overtone data. V_{eq} is independent of the hydrogen isotope. $(I_2/I_1)_M$ is the overtone-fundamental intensity ratio calculated from (5).

P-H or As-H bond in	ω_e (cm^{-1})	x_e ($\times 10^2$)	V_{eq} (eV)	$(I_2/I_1)_M$
PH;Zn	2375.33	1.844	3.99	0.019
PD;Zn	1710.22	1.337	3.97	0.014
PH;Cd	2417.16	1.751	4.28	0.018
PD;Cd	1739.23[a]	1.26[a]	4.28	0.013[a]
AsH;Zn	2224.12	1.735	3.97	0.018
AsD;Zn	1588.4[a]	1.24[a]	3.97	0.013[a]
$V_{In}(PH)_4$	2399.25	1.743	4.28	0.018

[a]Calculated.

the *X*-H atoms and III-V atom distances: The P-H bond is smaller than the As-H bond, but the relaxed P...Zn structure is longer than the As...Zn structure. Therefore, the H atom is less compressed in InP than in GaAs and this must allow for more anharmonicity of its vibration in InP. This seems to be confirmed by the reduction of x_e for P-H;Cd because of the confinement produced by the Cd atom that is larger than Zn. The anharmonicity parameters of the P-H bond associated with the 2316-cm^{-1} line could be measured up to 200 K and for this particular bond, x_e is found to be the same as at 6 K. The overtone to fundamental intensity ratios predicted from expression (5) can be estimated from the x_e values in Table V and they are larger than the experimental ones (Table I). Differences between the calculated and experimental intensity ratios have been observed for different OH^- oscillators and they have been attributed to the electrical anharmonicity of the dipole moment.[35,36] In the case of OH^- in CsCl, the intensity ratios calculated using (5) are smaller than the experimental ratio by a factor of 200, but for the same oscillator in NaF:Mg, the calculated ratio is larger by a factor of 2 than the experimental one. Detailed calculations of the dependence of the dipole moments of the OH^- and SH^- oscillators on the interatomic distance exist,[37] but not for PH, and the present work can stimulate such a study for PH and AsH oscillators.

3. *Comparison with the parameters deduced from the isotropic combinations*

When one atom of an *X*H oscillator is replaced by an isotope, expression (4) reads

$$\omega[XH]_i(v)=R\omega_e(v+\tfrac{1}{2})-R^2\omega_e x_e(v+\tfrac{1}{2})^2 , \qquad (6)$$

where $R^2=\mu/\mu_i$. When the frequencies of the fundamentals for *X*H and for $[XH]_i$ are known, one can also calculate anharmonicity parameters independently in the isolated oscillator approximation (IOA), i.e., for bare reduced masses. In this approximation, the values of x_e for Be, Zn, and Cd acceptors in GaAs and InP are given in Table VI. The values of x_e (V_{eq}) obtained in this way are generally larger (smaller) than the ones derived from the overtone measurements.[38] This is because the interaction of the oscillator with its surroundings that was implicitly included in the former case is neglected in the latter. Therefore, it seems that the larger tne difference between the values of x_e determined by the two methods, the larger the interaction between the bond and the lattice. The relation between the x_e derived in the IOA and the FWHP's must be considered with care when comparing centers with different structures. For instance, from the published data[29] of proton- and deuteron-implanted InP:Fe, one can calculate x_e in the IOA for $V_{In}(PH)$ and $V_{In}(PH)_4$ at 77 K and the values should not differ greatly

TABLE VI. Anharmonicity parameters x_e and V_{eq} at 6 K calculated from the hydrogen isotopic shift with expression (7) in the isolated oscillator approximation.

P-H or As-H bond in	FWHP (cm^{-1})	x_e ($\times 10^2$)	V_{eq} (eV)	x_e(Table V)/x_e(Table VI)
PH;Be	0.43	2.606	2.81	
PH;Zn	0.23	2.247	3.30	0.821
PH;Cd	0.12	2.087	3.62	0.839
AsH;Be	3.6	2.444	2.72	
AsH;Zn	1.8	2.273	3.07	0.763
AsH;Cd	1.3	2.246	3.19	

at LHeT. The values are 0.0244 and 0.0214, respectively. When the value of 0.0214 for $V_{In}(PH)_4$ is compared with 0.0174 calculated from the overtone measurements (Table V), it seems that despite very small FWHP's, the coupling of these oscillators with their environment is by no mean negligible.

4. *Anharmonicity parameters and interaction of the oscillator with the crystal*

A value of μ/μ_i taking into account the interaction of the oscillator with the crystal can be derived from the experimental ratio

$$R_{exp}=\omega_1[XH]_i/\omega_1[XH]=R(1-2Rx_e)/(1-2x_e)\ , \quad (7)$$

using x_e obtained from the overtone measurements. Following the suggestion of Ref. 39, the reduced mass of the interacting oscillator is written

$$\mu_c[XH]^{-1}=(\chi M_X)^{-1}+(\chi_H M_H)^{-1} \quad (8)$$

for XH and a similar expression holds for $[XH]_i$, where M_X and M_H are the bare masses of the atoms. The parameters χ, χ_H (or χ_D) translate the interaction of the X and H atoms with the crystal into a change of their mass. When the interaction between hydrogen and the crystal is ignored, χ is calculated by solving (7) with respect to R. For AsH;Zn and PH;Zn, the values of χ so obtained are 0.64 and 0.85, respectively, from the XH and XD data. This seems to be unphysical as the mass of the X atom coupled to the crystal is expected to be greater than its bare mass. Once an interaction of hydrogen with the lattice is postulated, the fit needs an increase of χ and it is very sensitive to the ratio χ_H/χ_D. If we correlate the amplitude of vibration of the H atom to its coupling to the acceptor, then χ_H should be larger than χ_D. For the PH and AsH modes, it is not possible to determine separately χ and χ_H (or χ_D). It is found that (i) when χ_H/χ_D is fixed, χ is proportional to χ_H (or χ_D), (ii) χ_H, χ_H/χ_D, and χ vary in the same direction, and (iii) for fixed χ_H, an increase of χ_H/χ_D produces an increase of χ. The triplet $(\chi,\chi_H,\chi_H/\chi_D)$ fitting the calculated value is not unique. For instance, a value of $\chi=2$ will fit the pair $(\chi_H,\chi_H/\chi_D)$ for (1.03,1.0134) or (1.07,1.0131) for AsH;Zn and (1.03,1.0205) or (1.07,1.0195) for PH;Zn.

5. *The amplitudes of vibration*

For an anharmonic potential, the equilibrium position of the H atom is different from zero. The quantity considered here to be meaningful of the amplitude of the motion is the mean-square amplitude $\langle\xi^2(v)\rangle$. For a Morse potential expanded in a polynomial form to ξ^4 with harmonic-oscillator eigenfunctions corrected to the second order,[40]

$$\begin{aligned}\langle\xi_M(v)\rangle&=3\sqrt{2x_e}(2v+1)/4\ ,\\ \langle\xi_M^2(v)\rangle&=(v+\tfrac{1}{2})+x_e(46v^2+46v+15)/8\ .\end{aligned} \quad (9)$$

Table VII summarizes the results for the amplitude of vibration of the hydrogen atom for the first vibrational states derived from the overtone measurements using expressions (9). As expected, an increase of the mean amplitude of vibration with the anharmonicity is observed and the XH amplitudes are larger than the corresponding XD ones in both the harmonic and anharmonic approximations. It has been observed that the FWHP's of the PH and AsH modes are acceptor dependent or, for the native complexes, complex dependent. These dependences are related to the environment of the H atom. At the beginning of the discussion, the low-temperature FWHP was related to the screening. This certainly holds true for the fundamental. For the overtone, the mean amplitude of motion of the H atom increases and size effects can show up. This can explain why the FWHP of the PH;Cd overtone is twice as large as that of the PH;Zn overtone, whereas the order is inverted for the fundamental. For the acceptor complexes, the FWHP decreases when H is replaced by D. In that case, the environment is the same, but the amplitude of vibration is ~20% smaller for the D complex than for the corresponding H complex. A ratio of the FWHP's proportional to the ratio of the square of the mean-square displacements $\langle x_M^2\rangle^2$ would give an increase of ~2 of the FWHP be-

TABLE VII. Comparison of the anharmonic (index a) and harmonic (index h) amplitudes of vibration ($\times 10^2$ Å) at 6 K for different X-hydrogen oscillators in GaAs and InP (from the bottom $v=0$, 1, and 2). They are calculated from $x=\xi\ell$, using $\mu=1$ and 2 a.m.u. for XH and XD and the experimental frequency ω_1. $\langle x_a\rangle$ is the shift from the harmonic equilibrium position.

	X-hydrogen oscillator in				
	AsH;Zn	PH;Zn	PD;Zn	PH;Cd	$V_{In}(PH)_4$
$\langle x_a\rangle$	8.7	8.7	6.1	8.4	8.4
	5.2	5.2	3.7	5.0	5.1
	1.7	1.7	1.2	1.7	1.7
$\sqrt{\langle x_a^2\rangle}$	22.1	21.5	17.3	21.2	21.3
	16.4	16.1	13.0	15.8	15.8
	9.0	8.8	7.3	8.7	8.7
$\sqrt{\langle x_h^2\rangle}$	19.7	19.1	15.8	18.9	19.0
	15.3	14.8	12.3	14.7	14.7
	8.0	8.5	7.1	8.5	8.5

tween the PD and the corresponding PH mode. This is the order of magnitude of what is observed. The relationship between the FWHP's and the amplitudes of vibration in corresponding structures is confirmed from the study[38] of the OH^-, OD^-, and OT^- (T is for tritium) modes in rutile (TiO_2). In this compound, the OH^-/OD^- ratio of the FWHP is 3.3 and the OD^-/OT^- ratio is 1.9.

D. Analysis of the temperature-dependent effects

One contribution to the FWHP of an absorption line is the finite lifetime of the excited state. The *X*H oscillator can relax to the ground state by emission of lattice phonons, but for high-frequency modes, this process is not very efficient because of the relatively high number of phonons that must be emitted simultaneously (~ 7 to 8 for GaAs or InP). Another possibility is the emission of a photon, but the radiative lifetime for these states is not known.[41] During its lifetime in the excited state, the number of periods of an *X*H oscillator can be very large ($\sim 10^4$–10^5). It has been assumed that the width of the high-frequency line is actually controlled by the dephasing of the oscillation without deexcitation (random vibrational dephasing). This dephasing is caused by a temperature-dependent exchange interaction with the low-frequency excitations of the medium (lattice phonons or possible low-frequency excitations of the *X*H bond). From an analysis of the temperature shifts and broadenings of the stretching modes of C-H and C-D bonds of tetramethyl-benzene (durene) between 10 and 200 K using this model, it was found there that coupling occurred between the stretching modes and a low-frequency mode of the molecule with a quasiexcitonic character.[5] The temperature dependences of the SiH modes on (111) silicon surfaces and of bulk CH modes in GaAs have also been analyzed within this framework.[42,43] Sketchily, one starts from a high-frequency absorption of a *X*H stretching mode with a Lorentz profile peaked at ω_{eff} with a FWHP $\Gamma(T)$ at temperature T. When using the Bose-Einstein statistics for the quantum oscillators, the shift $\Delta\omega=\omega_{\text{eff}}-\omega_{\text{LT}}$ of the *X*H mode with frequency ω_{LT} near 0 K is

$$\Delta\omega=\delta\omega/[\exp(\omega_0/k_BT)-1], \quad (10)$$

where ω_0 is the frequency of the low-frequency mode with lifetime τ and $\delta\omega$ the coupling constant. The coupling constant $\delta\omega$ can be positive or negative depending on the repulsive or attractive nature of the interaction between the two modes. The increase $\Delta\Gamma=\Gamma(T)-\Gamma_0$ of the FWHP with temperature (Γ_0 is the residual FWHP near 0 K) is

$$\Delta\Gamma=2(\delta\omega)^2c\tau\exp(\omega_0/k_BT)/[\exp(\omega_0/k_BT)-1]^2 . \quad (11)$$

$\gamma=1/c\tau$ can be considered as the width of the low-frequency mode coupled to the *X*H mode. The two above expressions have been used to analyze the experimental data. The analysis is justified if $\delta\omega \ll \gamma$.

The temperature dependence of the frequencies and FWHP's of the PH;Zn and PD;Zn modes can be fitted with the same values $\omega_0=61\pm3$ cm^{-1} and $\gamma=45\pm5$ cm^{-1} but with interaction coefficients $\delta\omega_H$ and $\delta\omega_D$, respectively, equal to -3.8 and -2.9 cm^{-1}. The value of ω_0 is independent of the hydrogen isotope and we here identify ω_0 as the frequency of a TA phonon at the L point of the Brillouin zone.[44] For PH;Cd, a fit can be obtained for $\omega_0=50$ cm^{-1}, $\gamma=30$ cm^{-1}, and $\delta\omega=-5.0$ cm^{-1}. Here again, a TA phonon at the X point of the Brillouin zone seems to be the best candidate.

It is found that the fundamental $V_{\text{In}}(PH)_4$ mode couples to a mode ω_0 at 136 cm^{-1} with $\gamma=30$ cm^{-1} and an interaction constant of -2.6 cm^{-1}. This low-frequency mode can be ascribed to a 2TA(L)-phonon combination. Its overtone can be observed up to 150 K and the above analysis indicates a coupling with a 2TA(L) combination ($\omega_0=99$ cm^{-1}) with $\gamma=55$ cm^{-1} and $\delta\omega=-3$ cm^{-1}. The above fits are represented by the solid lines in Figs. 5 and 6 and they seem to give a fair representation of the temperature dependences.

The coupling of *BC* complexes of H with TA lattice phonons has been found for $C_{As}H$;Ga and $N_{As}H$;*X* in GaAs.[43,45] We do not know if this specific coupling can be correlated with the structure of the center. This is also true from the two-phonon combination that has been found here to be associated with centers involving a lattice vacancy. The value of γ is assumed to be related to the phonon or to the phonon combination mean lifetime τ. The values of τ derived from the vibrational dephasing model are of about 1 ps. This value is weighted in a broad temperature range so that it cannot be compared simply with a value obtained at a given temperature. The rather high value of γ can be also related to the contribution of phonons with a broad distribution of wave vectors. The above coupling model does not seem to be valid to describe the coupling of the *X*H mode with a high-frequency bending mode at frequencies within the TO-phonon range or higher because such a mode is a localized mode and this can be a pitfall of this model.

V. CONCLUSION

The trends in the frequencies and the FWHP's of the fundamental PH; acceptor stretch modes in InP are attributed to the size of the acceptor for the frequencies and to electronegativity differences for the FWHP's. The smaller FWHP's of the corresponding PD; acceptor modes are related to the smaller amplitude of vibration of the D atom.

Despite the fact that lines attributed to (H,Mn) and to (H,Ti) complexes[14] were not observed here, a great number of PH-related lines have been observed. Two lines related to PH-vacancy complexes have been identified with a reasonable certitude and another is due to a residual (H,Zn) complex. The existence of other sharp lines indicates the presence in InP:Fe of centers whose structures remain to be elucidated. The very weak and relatively broad lines at 2322 and 2333 cm^{-1} could be due to H complexes with residual heavy acceptors like Ag and Hg, but confirmation is needed. By comparison with the intensity of the PH;Zn mode that has been calibrated, the concentration of these complexes would be in the 10^{13}-cm^{-3} range.

The trigonal symmetry of the PH;Zn and PH;V_{In}(PH) centers is clearly identified and the negative piezospectroscopic coefficients of V_{In}(PH) are consistent with the presence of a vacancy in the center. The stress splitting of the line at 2316 cm^{-1} in InP:Fe indicates that this line is due to a triply degenerate PH mode in a center with cubic symmetry. It is identified with $V_{In}(PH)_4$. A vacancy "decorated" by four H atoms seems thus to be a stable structure in InP as well as in silicon. The 2316-cm^{-1} line is not observed, however, in LEC p-type material.[46] This could be explained by a Fermi-level dependence of the charge state of hydrogen: if only protons are present in the p-type material, covalent PH bonds will not form with V_{In}. Another possibility is the absence of In vacancies in p-type material because of the excess of indium.

Annealing at 600 °C of the as-grown InP:Fe samples used here has produced a decrease of the intensity of the $V_{In}(PH)_4$ mode and the growth of the V_{In}(PH) mode. This is consistent with the thermal dissociation of $V_{In}(PH)_4$ producing V_{In}(PH). This dissociation should also produce the intermediate species $V_{In}(PH)_3$ and $V_{In}(PH)_2$. Because of their symmetry, two distinct IR active PH modes are expected for each of these centers. The lines between 2250 and 2254 cm^{-1} and the 2273 cm^{-1} line have been observed after annealing the samples. These lines could be related to the $V_{In}(PH)_3$ or $V_{In}(PH)_2$ centers or to PH bonds associated with centers having captured H atoms released by the dissociation of $V_{In}(PH)_4$. More work is necessary to elucidate these possibilities. It must be pointed out that the annealing behavior of the H complexes in bulk InP:Fe samples, with an overall H concentrations of about 10^{16} cm^{-3}, is very different from that observed for implanted samples where the concentration is three orders of magnitude higher.[30] This is also true from the annealing behavior of the PH;Zn mode. The two kinds of data are thus difficult to compare significantly.

The PH bonds studied show a weak anharmonicity compared to the one in small molecules. The overtone-fundamental intensity ratios measured are two to four times smaller than the ones calculated with a Morse potential. Similar or larger differences in the intensities ratios have been observed for O-H bonds in other materials and they have been attributed to electrical anharmonicity. A comparison of the anharmonicity parameters x_e of the (hydrogen-acceptor) complexes obtained separately from the overtone data and from the isotopic shifts has been made. It gives evidence from the interaction between the hydrogen and acceptor atoms, but more experimental data are required to evaluate independently this interaction.

The temperature dependence of the frequency and of the FWHP of the PH modes has been analyzed by assuming that they were due to the random dephasing of the oscillator in the excited state. For the H- and D-acceptor centers studied, it is found that the dephasing is caused by TA phonons. This same conclusion has been reached for other H-related complexes. For the V_{In}(PH) and $V_{In}(PH)_4$ modes, the dephasing is due to a 2TA-phonon combination.

ACKNOWLEDGMENTS

We wish to thank C. Naud and C. Song for their help in the experiments and the processing of the data. The InP:Fe cones were kindly provided by J. P. Farges and one InP:Fe sample was provided by B. Clerjaud. We are also grateful to J. P. Liévin and to D. Rondi for providing some p-type InP wafers. The samples were competently processed by M. Lemal and N. Lenain. Accurate SIMS experiments were performed by M. Gauneau. We gratefully acknowledge valuable discussions with B. Clerjaud and D. Côte. Groupe de Physique des Solides and Laboratoire AOMC are Unités Associées Nos. 17 and 800 au CNRS, respectively.

[1]See, for instance, *Hydrogen in Semiconductors,* edited by J. I. Pankove and N. M. Johnson (Academic, Orlando, 1991).

[2]J. Chevallier, B. Clerjaud, and B. Pajot, in *Hydrogen in Semiconductors,* Ref. 1, p. 447.

[3]B. Pajot, B. Clerjaud, and J. Chevallier, Physica B **170**, 371 (1991).

[4]A. Baurichter, M. Deicher, S. Deubler, D. Forkel, J. Meier, and W. Witthuhn, in *Defects in Semiconductors 16,* edited by G. Davies, M. Stavola, and G. DeLeo, Materials Science Forum Vol. 83-87 (Trans Tech, Aedermannsdorf, 1992), p. 593.

[5]C. B. Harris, R. M. Shelby, and P. A. Cornelius, Phys. Rev. Lett. **38**, 1415 (1977).

[6]B. N. Personn and R. Rydberg, Phys. Rev. B **32**, 3586 (1985).

[7]J. Chevallier, A. Jalil, B. Theys, J. C. Pesant, M. Aucouturier, B. Rose, and A. Mircea, Semicond. Sci. Technol. **4**, 87 (1989).

[8]L. M. Sverdlov, M. Kovner, and E. P. Karainov, *Vibration Spectra of Polyatomic Molecules* (Wiley, New York, 1974).

[9]K. P. Huber and G. Herzberg, *Constants of Diatomic Molecules,* Molecular Spectra and Structures, Vol. IV (Van Nostrand Reinhold, New York, 1979).

[10]B. Pajot, J. Chevallier, A. Jalil, and B. Rose, Semicond. Sci. Technol. **4**, 91 (1989).

[11]R. Rahbi, B. Pajot, J. Chevallier, A. Marbeuf, R. C. Logan, and M. Gavand, J. Appl. Phys. **73**, 1723 (1993).

[12]R. Darwich, B. Pajot, B. Rose, D. Robein, R. Rahbi, and B. Theys, in *Proceedings of the XXI International Conference on the Physics of Semiconductors,* edited by Pin Jiang and Hou-Zhi Zheng (World Scientific, Singapore, 1992), p. 1709.

[13]M. O. Manasreh (private communication).

[14]B. Clerjaud, D. Côte, and C. Naud, Phys. Rev. Lett. **58**, 1755; J. Cryst. Growth **83**, 190 (1987).

[15]M. Stavola, S. J. Pearton, J. Lopata, and W. C. Dautremont-Smith, Phys. Rev. B **37**, 8313 (1988).

[16]B. Pajot and C. Y. Song, Phys. Rev. B **45**, 6484 (1992).

[17]R. Darwich, B. Pajot, C. Y. Song, B. Rose, B. Theys, and C. Porte, in *20th International Conference on the Physics of Semiconductors,* edited by E. M. Anastassakis and J. D. Joannopoulos (World Scientific, Singapore, 1990), p. 791.

[18]B. Clerjaud, Physica B **170**, 383 (1991).

[19]N. M. Johnson, R. D. Burnham, R. A. Street, and R. L. Thornton, Phys. Rev. B **33**, 1102 (1986).

[20]B. Pajot, A. Jalil, J. Chevallier, and R. Azoulay, Semicond. Sci. Technol. **2**, 305 (1987).

[21]A. A. Kaplianskii, Opt. Spektrosk. **16**, 602 (1964) [Opt. Spectrosc. (USSR) **16**, 329 (1964)].
[22]M. Stavola, S. J. Pearton, J. Lopata, C. R. Abernathy, and K. Bergman, Phys. Rev. B **39**, 8051 (1989).
[23]K. Bergman, M. Stavola, S. J. Pearton, and T. Hayes, Phys. Rev. B **38**, 9643 (1988).
[24]B. Bech-Nielsen, J. Olajos, and H. G. Grimmeiss, Phys. Rev. B **39**, 3330 (1989).
[25]B. Bech-Nielsen (private communication).
[26]T. S. Shi, L. M. Xie, G. R. Bai, and M. W. Qi, Phys. Status Solidi B **131**, 511 (1985).
[27]G. Herzberg, *Infrared and Raman Spectra of Polyatomic Molecules,* Molecular Spectra and Molecular Structure, Vol. II (Krieger, Malabar, FL, 1991).
[28]J. Tatarkiewicz, B. Clerjaud, D. Côte, F. Gendron, and A. M. Hennel, Appl. Phys. Lett. **53**, 382 (1988).
[29]D. W. Fischer, M. O. Manasreh, and G. Matous, J. Appl. Phys. **71**, 4805 (1992).
[30]D. W. Fischer, M. O. Manasreh, D. N. Talwar, and G. Matous, J. Appl. Phys. **73**, 78 (1993).
[31]B. Pajot, C. Song, and C. Porte (unpublished).
[32]G. Herzberg, *Spectra of Diatomic Molecules,* Molecular Spectra and Molecular Structure, Vol. I (Van Nostrand, Princeton, 1950).
[33]J. E. Rosenthal, Proc. Nat. Acad. Sci. U.S.A. **21**, 281 (1935).
[34]D. C. McKean, I. Torto, and A. R. Morrisson, J. Phys. Chem. **86**, 307 (1982).
[35]M. Krantz and F. Lüty, Phys. Rev. B **37**, 7038 (1988).
[36]W. Beall Fowler, R. Capelletti, and E. Colombi, Phys. Rev. B **44**, 2961 (1991).
[37]P. E. Cade, J. Chem. Phys. **47**, 2390 (1967).
[38]J. B. Bates and R. A. Perkins, Phys. Rev. B **16**, 3713 (1977).
[39]R. C. Newman, Physica B **170**, 409 (1991).
[40]A. Reitan, K. Nor. Vidensk. Selsk. Skr. **2**, 1 (1958).
[41]The lifetime of the excited states of the SiH surface mode on ideally H-terminated silicon (111) surfaces has been measured to be ~ 1 ns [P. Guyot-Sionnest, P. Dumas, Y. J. Chabal, and G. S. Higashi, Phys. Rev. Lett. **18**, 2156 (1990)].
[42]P. Dumas, Y. J. Chabal, and G. S. Higashi, Phys. Rev. Lett. **65**, 1124 (1990).
[43]B. Clerjaud, D. Côte, F. Gendron, W. Hahn, M. Krause, C. Porte, and W. Ulrici, in *Defects in Semiconductors 16,* edited by G. Davies, M. Stavola, and G. DeLeo, Materials Science Forum Vol. 83-87 (Trans Tech, Aedermannsdorf, 1992), p. 563.
[44]The frequencies of the TA(L), TA(X), 2TA(L), and 2TA(X) phonons in InP are 55, 69, 110, and 137 cm^{-1}, respectively [M. Vandevyver and P. Plumelle, J. Phys. Chem. Solids **38**, 765 (1977)].
[45]C. Song, thesis, University Paris 7, 1992.
[46]B. Clerjaud (private communication).